Internal Report Number 14

GAMMA-RAY PRODUCED BACKGROUND IN $e^{\pm}$ GONDOLA

C. RICE

January, 1970

In this report we estimate the contribution of gamma-ray induced background events to the measured electron intensity at float altitude for the $e^{\pm}$ gondola. The most significant potential source is the lucite Čerenkov counter which can produce spurious events in the manner shown schematically in Figure 1. A photon which interacts in the counter may produce a negatron by Compton scattering or a negatron-positron pair by materialization. A resultant electron may trigger the Čerenkov counter and subsequently scatter into the acceptance cone where it triggers counters T1 and T2. Since the electron is traveling backward through the spectrometer, the assigned charge for the event will be the opposite of the true charge of the particle. In the following discussion we shall use incident angles Θ and ϕ for the γ-ray, where Θ is measured from the nadir (negative z-axis) and ϕ is measured from the positive y-axis in a right-handed coordinate system. (See Figure 2 for the orientation of the reference cartesian coordinate system).

We let $F_\gamma\ (E_\gamma,\Theta)$ represent the differential γ-ray flux at float altitudes at a γ-ray energy of E_γ. The background contribution to the measured positron and negatron fluxes in the i^{th} energy interval ΔE^i is then

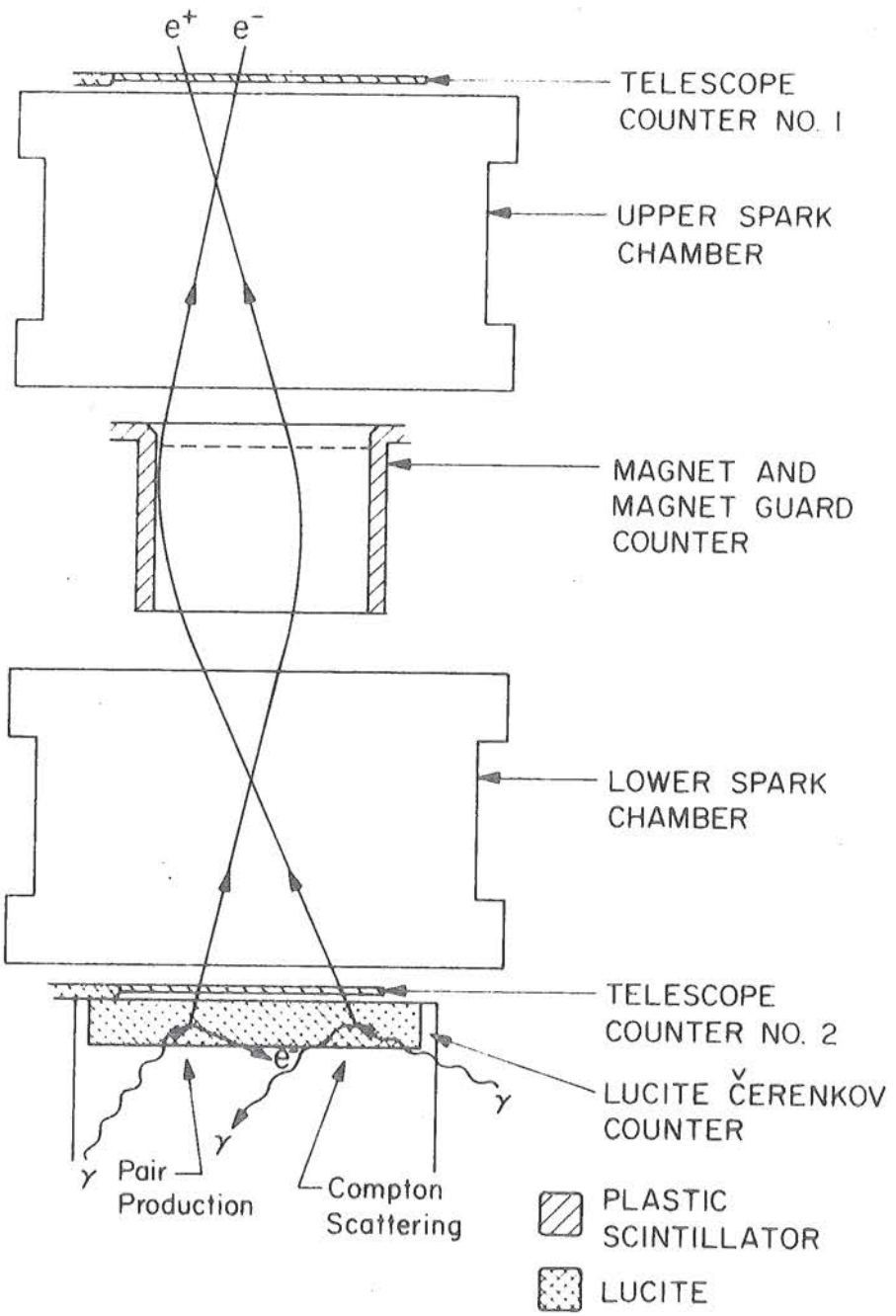

Fig. 1. Schematic representation of gamma-ray interactions in the lucite Čerenkov counter which can produce spurious electron events. The interactions involved are Compton scattering and pair production. Path marked e^+ will be registered as e^- and vice versa due to the backward trajectory.

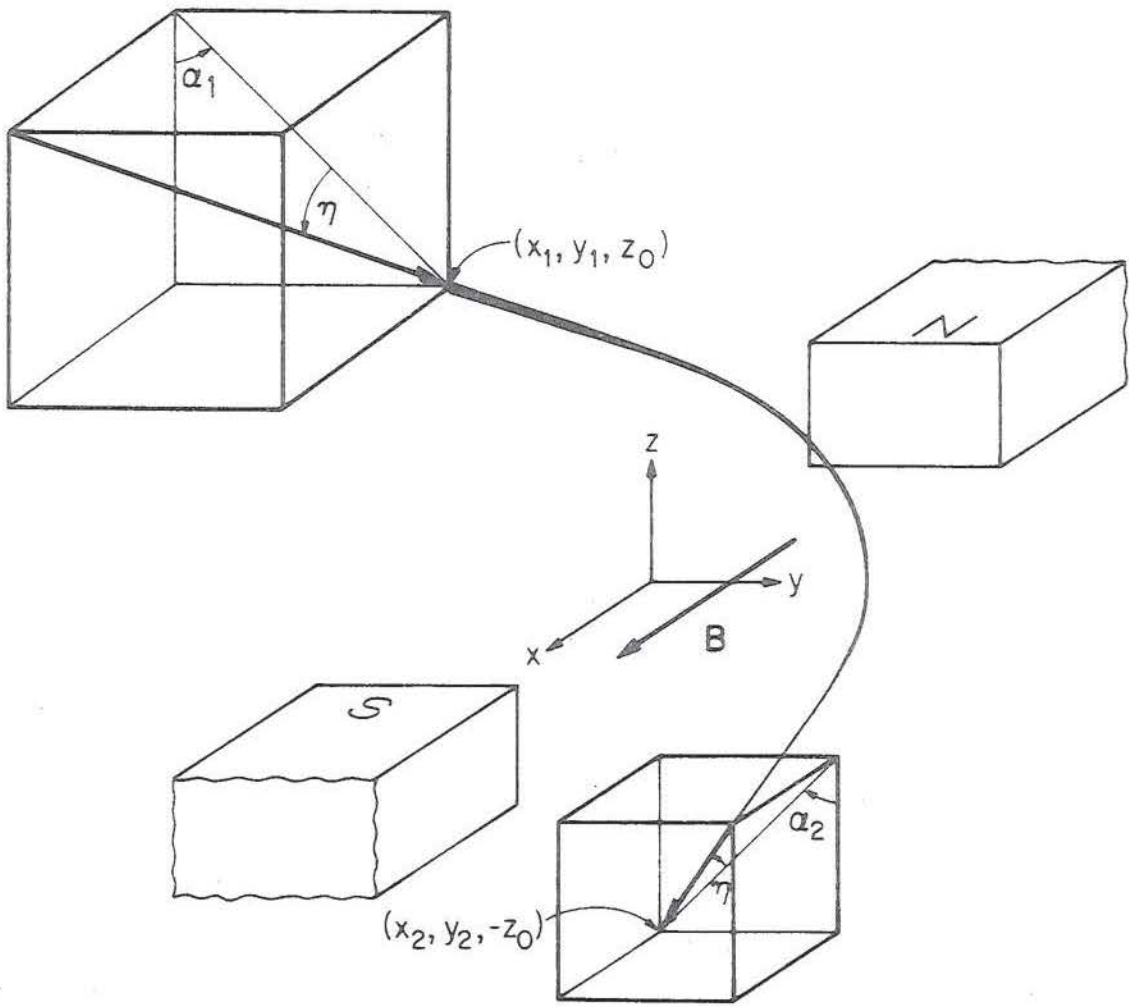

Fig. 2. Schematic view of a particle trajectory through the magnet gap, showing reference coordinate system and trajectory parameters used in the calculation of the particle rigidity.

$$F_{\pm}^{B}(\Delta E^{i}) = \frac{1}{\Delta E^{i} G_{i}} \int_{\Delta E^{i}} dE \int_{E}^{\infty} dE_{\gamma} \int_{4\pi} d\Omega \int_{A} dA \; T_{\pm}(E,E_{\gamma},\Theta,\phi,x,y) F_{\gamma}(E_{\gamma},\Theta) \tag{1}$$

where G_i is the geometrical factor of the detector for the electron energy interval ΔE, $d\Omega$ an element of solid angle, A the area of the Čerenkov counter radiator, and $T_{\pm}$ the probability that a γ-ray of energy E_{γ} incident on the counter at location x, y with incident angles Θ and ϕ will produce a negatron or position which will trigger the detector and be analyzed as a positron or negatron of energy E. In general $T_{+} \neq T_{-}$. Since negatrons are produced by both Compton scattering and pair production, while positrons result only from the latter we would expect that

$$T_{+}(E,E_{\gamma},\Theta,\phi,x,y) \geq T_{-}(E,E_{\gamma},\Theta,\phi + 180^{o},-x,-y) \tag{2}$$

At higher γ-ray energies the Compton process becomes less important and eq. (2) will approach the equality.

With a very narrow, intense, mono-energetic γ-ray beam and sufficient time it would be possible to determine $T_{\pm}$ precisely. Experimental limitations at the California Institute of Technology Sychrotron Laboratory, where we carried out the calibrations, required several compromises. Although a tagged photon beam was available, its intensity was far too low for our purposes. We therefore used a bremsstrahlung beam from 300 MeV electrons incident on a 1/8" Copper radiator. The differential energy spectrum of the bremsstrahlung beam was calculated using the computer program BPAKI (1). The γ-ray flux incident on a one-inch square at the location of our Čerenkov counter and centered on the original trajectory of the radiating

electron is $S(E_\gamma) \approx 1.16\times10^{-2}\ E_\gamma^{-1.22}$ photons per electron per MeV. This is about 85 percent of the total radiated photon flux. Quoted accuracy of the program is about 2 percent. We shall use this value of $S(E_\gamma)$ as an average value. The experimental setup was such that this will perhaps slightly overestimate the sensitivity of the detector to γ-ray produced events. The original electron beam itself is several centimeters wide at the location of our Čerenkov counter. This is wide enough to essentially average over x and y. We denote the relative photon intensity at x',y' (in a plane normal to the incoming electron beam and with the coordinate origin at the center of the beam) by the function P(x',y') normalized such that

$$\int_{-\infty}^{\infty}\int_{-\infty}^{\infty} P(x',y')\,dx'dy' = 1$$

The quantity which is measured during an exposure is the number of positrons and negatrons $N_\pm$ detected in the i^{th} energy interval for a given number n_e of electrons incident on the copper radiator. $N_\pm$ is measured for many different incident angles (Θ_ℓ,ϕ_ℓ). In terms of eq. (1) we have

$$N_\pm\ (\Delta E,\Theta_\ell,\phi_\ell) =$$

$$= \int_{\Delta E^i} dE \int_{E}^{\infty} dE_\gamma \int_{\Omega} d\Omega \int_{A'} dA\ \ T_\pm\ (E,E_\gamma,\Theta,\phi,x,y)\ n_e^\ell S(E_\gamma)\delta(\Theta_\ell)\delta(\phi_\ell)P(x',y') \qquad (3)$$

In the above equation A' is the projected area of the Čerenkov counter normal to the incoming beam; the relationship of x, y, and x',y'

is determined by the location of the counter in the beam.

Using the measured values $N_{\pm}$ and eq. (2), we can approximate $T_{\pm}$ averaged over x, y, valid for the energy interval ΔE^i and for angles near Θ_ℓ, ϕ_ℓ by

$$T_{\pm} \approx \tau_{\pm} (\Delta E^i, \Theta_\ell, \phi_\ell, \varepsilon_\gamma^{i\ell}) = \frac{N_{\pm} (\Delta E^i, \Theta_\ell, \phi_\ell)\, \delta(E_\gamma - \varepsilon_\gamma^{i\ell} (\Delta E^i, \Theta_\ell, \phi_\ell))}{\Delta E^i\, n_e^\ell S(E_\gamma) \int_{A'} P(x', y') dA'} \qquad (4)$$

where $\delta(E_\gamma - \varepsilon_\gamma)$ is a delta function and $\varepsilon_\gamma^{i\ell}$ is the mean energy of the photons which contribute to producing the detected positrons and negatrons in ΔE^i. The dependence of $\varepsilon_\gamma^{i\ell}$ on Θ_ℓ, ϕ_ℓ arises because the amount of scattering of the γ-ray produced electron required to enter the acceptance cone of the detector depends on these parameters. A large scattering simplies a longer path length and consequent greater energy loss in the lucite. There may also be a dependence on the charge of the detected particle. For a fixed electron energy in the detector the charge dependence would result from different mean energies of the interacting photons depending on whether the pair production or Compton process were involved. Since the choice of $\varepsilon_\gamma^{i\ell}$ is somewhat arbitrary in any case, we have chosen to ignore the charge dependence. The necessity of using $\varepsilon_\gamma^{i\ell}$ arises because of the use of the bremsstrahlung beam and because of limited time and beam intensity. At best, $\varepsilon_\gamma^{i\ell}$ can only be roughly estimated. On the other hand, as will be seen later, the dependence of the result on the choice of $\varepsilon_\gamma^{i\ell}$ is not strong. We will present estimated background fluxes during cosmic-ray observations using a variety of choices

for $\varepsilon_\gamma^{i\ell}$.

We now break up the solid angle and approximate both $F_\gamma(E_\gamma,\Theta)$ and $N_\pm\ (\Delta E^i,\Theta,\phi)$ over the entire interval $\Delta\Omega_\ell$ centered on Θ_ℓ,ϕ_ℓ values at Θ_ℓ,ϕ_ℓ. We can then write eq. (1), substituting $\tau_\perp$ for T_+, as

$$F_\pm^B\ (\Delta E^i) \approx \frac{1}{\Delta E^i G_i} \sum_\ell \frac{N_\pm(\Delta E^i,\Theta_\ell,\phi_\ell)}{n_e^\ell} \int_E^{300\ \mathrm{MeV}} dE_\gamma \frac{F_\gamma(E_\gamma,\Theta_\ell)}{S(E_\gamma)} \delta(E_\gamma-\varepsilon_\gamma^{i\ell}(\Delta E^i,\Theta_\ell,\phi_\ell))$$

$$\times \frac{\int_{\Delta\Omega_\ell} d\Omega \int_{A'} dA}{\int_{A'} P(x',y')dA'}$$

$$= \frac{1}{\Delta E^i G_i} \sum_\ell \frac{N_\pm(\Delta E^i,\Theta_\ell,\phi_\ell)\quad F_\gamma(\varepsilon_\gamma^{i\ell},\Theta_\ell)\ (A'\Delta\Omega_\ell)_\ell}{n_e^\ell\ S(\varepsilon_\gamma^{i\ell}) \int_{A'} P(x',y')dA'} \qquad (5)$$

where $(A'\Delta\Omega_\ell)_\ell$ is the projected area A' of the Cerenkov counter times the solid angle $\Delta\Omega_\ell$ for the ℓ^{th} interval.

The γ-ray spectrum at balloon altitudes for several incident angles from the zenith has been measured by Fichtel, Kniffen, and Ögelman (2). The observations were made at Mildura, Victoria, Australia in December, 1966. Although these data were gathered at a location with a much higher geomagnetic cutoff rigidity, 4.7 GV (3), than Fort Churchill, the level of solar modulation was also considerably less than in 1968. Comparison of the pion production curves of Perola

and Scarsi (4) indicate that these two effects are roughly compensatory. We therefore use the γ-ray spectra of Fichtel, et al. for Fort Churchill in 1968. In Figure 3A we show their integral γ-ray flux above 100 MeV as a function of incident angle from the nadir (note that this convention differs from that employed in the original publication). Figure 3B shows that the measured integral spectrum between 30 and 200 MeV for $\Theta = 16^{o}$ and 68^{o} can be well approximated by the power laws $.67\ E^{-1.15}$ and $.28\ E^{-.65}$, respectively. To estimate the spectra for other values of Θ we proceed in the following way. We use the curve drawn through the measured points in Figure 3A to fix the integral flux for $E > 100$ MeV. The power law approximations for $\Theta = 16^{o}$ and 68^{o} both pass through 930 photons/(cm^2.sr.sec) at $E = 5.6$ MeV. We artificially make the power law approximations for all $\Theta < 90^{o}$ pass through this point. (For $\Theta > 90^{o}$ the detector γ-ray sensitivity is essentially zero and we shall not consider this region in the subsequent analysis). The actual behavior of the γ-ray spectra below about 20 MeV has little effect on our estimate of the electron background and this choice is a convenient way of producing reasonable spectra at higher energies. The integral flux above 30 MeV derived by this method is shown as a function of Θ in Figure 3A and Table 1 gives the spectra derived for the nine values Θ_ℓ used in the summation of eq. (4).

If we substitute for $F_\gamma(E_\gamma,\Theta_\ell)$ in eq. (4) power laws of the form

$$F_\gamma(E_\gamma,\Theta_\ell) = B_\ell\ E_\gamma^{-\alpha_\ell}$$

and remember that $S(E_\gamma)$ has the form

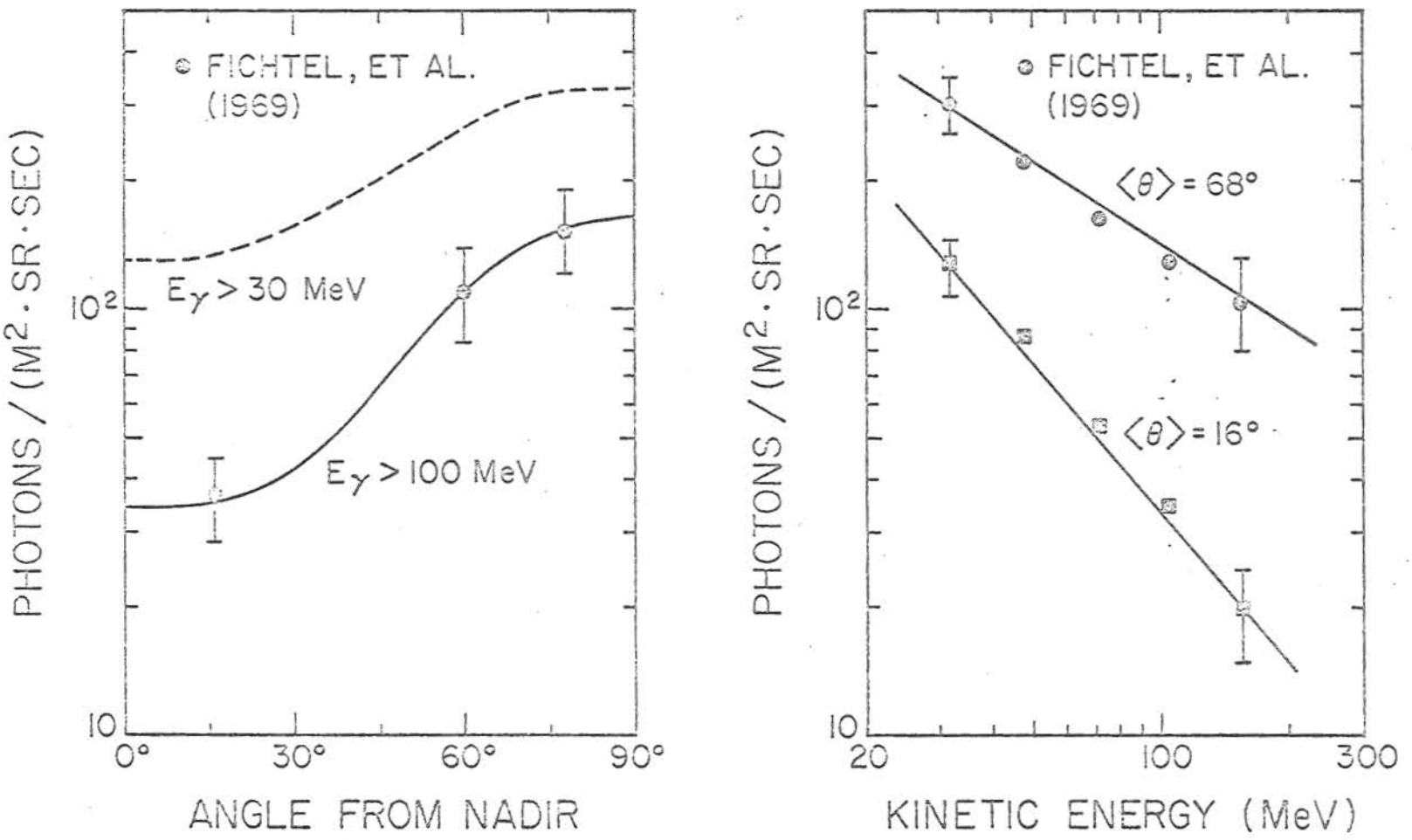

Fig. 3. Integral gamma-ray flux at balloon altitude as a function of angle and energy. Derivation of the angular distribution for $E_\gamma > 30$ MeV is described in the text.

TABLE 1

GAMMA-RAY SPECTRA

Gamma-ray spectra at different angles from the nadir as used in background calculation. See text for the method of derivation.

Angle from Nadir	Integral photon spectrum	Differential photon spectrum
$0<\theta<25^{o}$	$.67\ E^{-1.15}$	$.77\ E^{-2.15}$
$25^{o}<\theta<35^{o}$	$.61\ E^{-1.08}$	$.66\ E^{-2.08}$
$35^{o}<\theta<45^{o}$	$.51\ E^{-.98}$	$.50\ E^{-1.98}$
$45^{o}<\theta<55^{o}$	$.40\ E^{-.85}$	$.34\ E^{-1.85}$
$55^{o}<\theta<65^{o}$	$.33\ E^{-.74}$	$.24\ E^{-1.74}$
$65^{o}<\theta<75^{o}$	$.28\ E^{-.65}$	$.18\ E^{-1.65}$
$75^{o}<\theta<90^{o}$	$.27\ E^{-.62}$	$.17\ E^{-1.62}$

$$S(E_\gamma) = C\, E_\gamma^{-1.22}$$

we can simplify eq. (4) to

$$F_\pm^B(\Delta E^i) \approx \frac{1}{\Delta E^i G_i} \sum_\ell \frac{N_\pm(\Delta E^i, \Theta_\ell, \phi_\ell)\, B_\ell\, (A'\Delta\Omega_\ell)_\ell}{n_e^\ell\, C \int_{A'} P(x',y')dA'} \left(\varepsilon_\gamma{}^{i\ell}\right)^{-(\alpha_\ell - 1.22)}$$

$$= \sum_\ell f_{i\ell}^\pm\, B_\ell \left(\varepsilon_\gamma{}^{i\ell}\right)^{-(\alpha_\gamma - 1.22)} \qquad (6)$$

where

$$f_{i\ell}^\pm \equiv \frac{N_\pm(\Delta E^i, \Theta_\ell, \phi_\ell)\, (A'\Delta\Omega)_\ell}{\Delta E^i G_i n_e^\ell C \int_{A'} P(x',y')dA'}$$

The values $f_{i\ell}^\pm$ are functions of $\Delta E^i, \Theta_\ell, \phi_\ell$, and the charge sign, and are derived from data from the machine runs and other measured quantities. The choice of the ℓ intervals is determined by the machine data which is available. Our measurements cover the range of Θ from 0 to 90^o for both $\phi = 0$ and $\phi = 90^o$. We have data at $\phi = 180^o$ for only a few values of Θ. Detection of γ-ray produced positrons (registered as negatrons) is favored for $\phi = 0$, and the data for $\phi = 180$ is necessary to determine the relative number of positrons and negatrons produced in a given energy interval ΔE^i. Lack of these measurements means that this number must be estimated. For the purpose of the summation we have divided the hemisphere

centered on the nadir into 36 intervals: 9 divisions in Θ and 4 in ϕ. The nine intervals in Θ are listed in Table 1. The values of $f^{\pm}_{i\ell}$ measured at $\phi = 90^{o}$ are used in intervals of 120^{o} centered about $\phi = 90^{o}$ and $\phi = 270^{o}$; the values of $f^{\pm}_{i\ell}$ measured at $\phi = 0^{o}$ are used in the 60^{o} interval centered on $\phi = 0^{o}$. For the 60^{o} interval centered on 180^{o} we have also used the $f^{\pm}_{i\ell}$ measured at $\phi = 0^{o}$ but weighted according to the relative production number of positrons and negatrons. In particular, if the relative number of γ-ray produced positrons and negatrons at $\phi = 0^{o}$ is n^{+} and n^{-} respectively then

$$f^{\pm}_{i\ell}\ (\Theta,\phi = 180^{o}) \ = \ \frac{n^{\mp}}{n^{\pm}}\ f^{\mp}_{i\ell}\ (\Theta,\phi = 0^{o})$$

since positrons are detected as negatrons and vice versa.

The estimate of the values $n^{\pm}$ is related to the estimate of $\varepsilon_{\gamma}{}^{i\ell}$. The ratio of the probabilities for Compton collision μ_{comp} and for pair production μ_{pair} are approximately 1.5, 1, .5, .4, and .2 for E_{γ} = 20, 30, 40, 50, and 100 MeV respectively (5). Use of these values to estimate $\frac{n^{-}}{n^{+}}$ does not take into account the different energy spectra of the electrons produced in the two processes, but this neglect probably does not significantly effect our results. Internal evidence from the few machine runs available at $\phi = 180^{o}$ indicates that the ratio at low Θ and low electron energies is not more than 1.5 and may be considerably less. At larger Θ and higher energies the ratio should decrease since $\varepsilon_{\gamma}{}^{i\ell}$ should be greater. We choose the value

$$\frac{n^{-}}{n^{+}} \ = \ (\mu_{comp} + .5\ \mu_{pair})/.5\ \mu_{pair}$$

appropriate to the estimated value of $\varepsilon_\gamma^{i\ell}$. $F_\pm^B$ has been evaluated for several choices of $\varepsilon_\gamma^{i\ell}$ and the results are tabulated in Table 2. Where 3 values of ε_γ are indicated, they apply to the Θ intervals $0\text{-}25^o$, $25^o\text{-}55^o$, and $55^o\text{-}90^o$, respectively. Also listed are the estimated best values and error limits which are plotted in Figure 4.

The above analysis is limited in several respects which we have tried to point out at the appropriate places in the discussion. In addition, the measured values of $f_{i\ell}^\pm$ have relatively low statistical accuracy and do not cover as wide a range of ϕ as would be desirable. The chief effect of the choice of $\varepsilon_\gamma^{i\ell}$ comes from the resultant ratio n^-/n^+. Further machine runs have been undertaken which should improve this situation, both by providing values of $f_{i\ell}^\pm$ for $\phi = 180^o$ and by improved statistical accuracy.

TABLE 2

GAMMA-RAY PRODUCED POSITRON AND NEGATRON BACKGROUND

Background flux in the electron energy intervals 6-12 MeV, 12-25 MeV, and 25-50 MeV for various choices of ε_γ. Estimated best values and error limits are also given. ε_γ and $F_\pm^B$ are in units of MeV and $(M^2.sec.sr.MeV)^{-1}$, respectively.

6-12 MeV			12-25 MeV			25-50 MeV		
ε_γ	F_+^B	F_-^B	ε_γ	F_+^B	F_-^B	ε_γ	F_+^B	F_-^B
20	.18	.15	30	.068	.032	70	.0069	.0075
30	.12	.12	40	.048	.027	80	.0062	.0068
40	.083	.098	50	.039	.023	90	.0055	.0062
50	.068	.088	60	.033	.021	100	.0050	.0057
20-30-40	.13	.13	30-40-50	.057	.030	60-70-80	.0075	.0081
30-40-50	.087	.10	40-50-60	.044	.025	70-80-90	.0067	.0072
40-50-60	.071	.089	50-60-70	.036	.022	80-90-100	.0059	.0065
Estimated best values and error limits	.09 ±.09	.10 ±.06		.044 ±.030	.025 ±.010		.0059 ±.0030	.0066 ±.0030

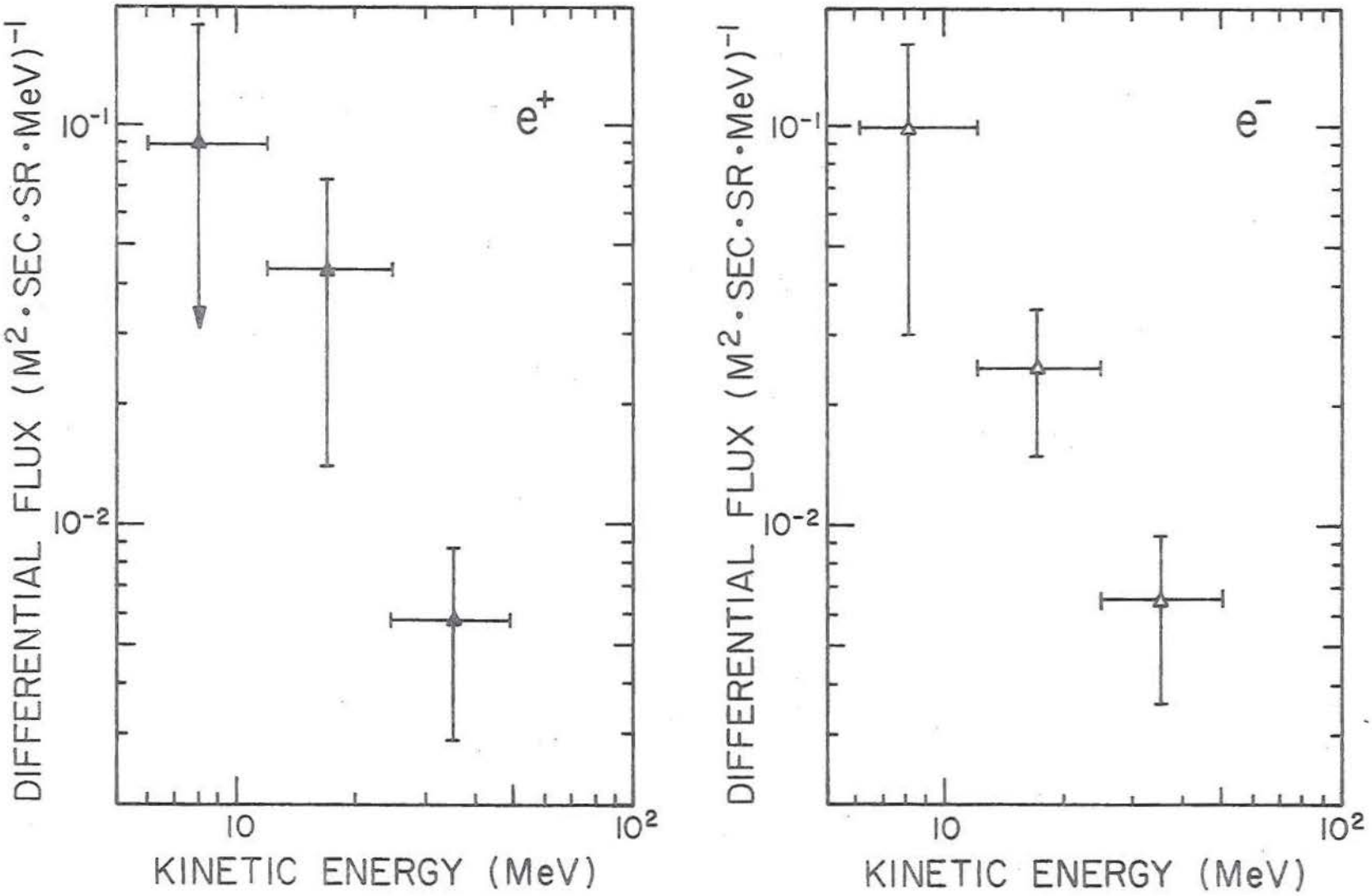

Fig. 4. Gamma-ray produced contribution to measured positron and negatron differential kinetic-energy spectra at balloon altitudes.

References

1. F. Wolverton, California Institute of Technology Synchrotron Laboratory, Private Communication.

2. C. E. Fichtel, D. A. Kniffen, and H. B. Ögelman, Astrophys. J. 158, 1963 (1969).

3. M. A. Shea, D. F. Smart, and J. R. McCall, Can. J. Phys. 46, 1098 (1968).

4. G. C. Perola and L. Scarsi, Nuovo Cimento 46, 718 (1966).

5. B. Rossi, High Energy Particles, (Prentice-Hall, Englewood Cliffs, N. J., 1952).